

Dynamic and Static Energy Efficient Design of Pinching Antenna Systems

Saba Asaad
University of Toronto
saba.asaad@utoronto.ca

Chongjun Ouyang
Queen Mary University
c.ouyang@qmul.ac.uk

Ali Bereyhi
University of Toronto
ali.bereyhi@utoronto.ca

Zhiguo Ding
Nanyang Technological University
zhiguo.ding@ntu.edu.sg

Abstract—We study the energy efficiency of pinching-antenna systems (PASSs) by developing a consistent formulation for power distribution in these systems. The per-antenna power distribution in PASSs is not controlled explicitly by a power allocation policy, but rather implicitly through tuning of pinching couplings and locations. Both these factors are tunable: (i) pinching locations are tuned using movable elements, and (ii) couplings can be tuned by varying the effective coupling length of the pinching elements. While the former is feasible to be addressed dynamically in settings with low user mobility, the latter cannot be addressed at a high rate. We thus develop a class of hybrid dynamic-static algorithms, which maximize the energy efficiency by updating the system parameters at different rates. Our experimental results depict that dynamic tuning of pinching locations can significantly boost energy efficiency of PASSs.

I. INTRODUCTION

Following the DOCOMO demonstration in [1], pinching-antenna systems (PASSs) have been proposed as a new technology to realize an analog front-end with flexible-antenna arrays [2]. A PASS consists of a long dielectric waveguide in which electromagnetic (EM) waves propagate with minimal attenuation. The EM signal is radiated from this waveguide using the so-called *pinching elements* which are freely moving across the waveguide [3]. The long scale of the waveguide allows the elements to place close to users and thereby drastically reduce the path-loss [3], [4]. Early studies on PASS have shown that by optimally placing and activating pinching elements, one can push the system toward a *near-wired* behavior, where the path-loss is dominated by the free-space propagation at the *last-meter* transmission [2]. Motivated by its high degrees of freedom, several recent lines of work have investigated design aspects of PASS. The work in [5] and [6] studies the integrability of this technology to multiple-input multiple-output (MIMO) systems, developing low-complexity algorithms for hybrid uplink and downlink beamforming with PASS. The study in [7] characterizes several performance metrics under realistic waveguide attenuation and path-loss models. Enhancing physical layer security using the high flexibility of PASSs is studied in [8].

A. Energy Efficiency of PASS

Due to its low-loss nature, PASSs are generally considered to have high energy efficiency (EE). Motivated by this intuitive

observation, a few recent studies have investigated the EE of PASSs, e.g. [9], [10]. The lines of work in this respect consider a classical power distribution model for PASSs. This means that they implicitly treat each pinching element as if it is an active antenna whose radiated power can be fully controlled by the transmitter. Considering the EM radiation in waveguides, one can observe that this is not necessarily the case in PASSs [11]. In fact, the transmit power of each pinching element is explicitly described by its location and coupling characteristics, and hence is less controllable as compared with conventional movable-antenna technologies [12].

This work aims to develop a realistic formulation for EE in PASSs. Motivated by the study in [11], we formulate the energy consumption and power distribution in a PASS in terms of the pinching locations and couplings. The power allocation is then addressed implicitly in these systems through location and coupling tuning at the transmitter.

B. Contributions and Organization

In this work, we study both *dynamic* and *static* designs for energy efficient transmission in PASSs. Our key contributions are three-fold: (i) We model the EE of PASSs taking into account the EM propagation in these systems. We show that conventional formulation based on earlier power distribution models is not applicable to PASSs. In fact, the power allocation in these systems is implicitly controlled through tuning of the pinching couplings and locations. (ii) Using our EE model, we formulate energy-efficient transmission in PASSs. The design variables in this problem vary at different rates: while per-user power allocation can be tuned at symbol-level, the coupling coefficients of the elements can be tuned only statically. We hence consider two realistic design scenarios: (i) a *dynamic* scenario, in which both *user* power allocation and pinching locations are adjusted at the rate of network coherence, i.e., they change as users change their locations, and the coupling lengths of the elements are tuned statistically. (ii) A *static* case in which only the user power allocation is adjusted at the coherence rate, and the pinching locations and couplings are tuned for optimal *ergodic* EE. (iii) We develop a two-tier algorithmic framework, whose inner layer updates the dynamic variables at the coherence rate, while the outer layer tunes the static parameters. Through extensive numerical experiments, we validate our analysis. Our numerical experiments depict a significant throughput gain

This work was supported in part by the German Research Foundation (Deutsche Forschungsgemeinschaft - DFG).

achieved by dynamic tuning of pinching locations, suggesting high efficiency of PASSs in environment with slow dynamics, e.g. indoor settings with low user mobility.

II. SYSTEM MODEL

Consider a dielectric waveguide of length L with N pinching elements positioned along the x -axis at height a . Let $0 \leq x_n \leq L$ be the location of element $n \in [N]$. The coordinate of the pinching element n can hence be written as $\mathbf{p}_n = [x_n, 0, a]$. Due to physical restrictions, each of the two neighboring elements is distanced more than a minimum threshold Δ , i.e., $x_n - x_{n-1} \geq \Delta$. Element n is of length ℓ_n and performs as a signal illuminator that operates by coupling with the waveguide. In the sequel, we assume that x_n denotes the *end point* of the element n , often called its *effective location*, i.e., the point where signal radiates from. We further denote the location where the element starts coupling with the waveguide by $x_{0,n}$, i.e., $x_n = x_{0,n} + \ell_n$. For sake of simplicity, we consider the following assumptions: (1) The propagation loss in the waveguide is negligible. (2) The pinching elements and dielectric waveguide have the same refractive indices i_{ref} . (3) The length of the pinching elements is designed such that complete coupling occurs, i.e., the the coupled power completely transfers to the element and is radiated in open space. (4) There is no power reflection at the end of the waveguide, and the non-radiated power at the end of the waveguide is burned to heat. Note that this assumption is realistic, as in practice (as we shall see), with large enough number of pinching elements, this power is negligible.

The waveguide is connected to an access point (AP), which deploys this PASS along with time-division multiple access (TDMA) for downlink transmission in a multiple access channel with K users. For this setting, we aim to design the system parameters, i.e., the location of elements and their length, such that the EE is maximized, i.e., to maximize the average spectral efficiency achieved per unit of power. This requires a concrete characterization of energy consumption in this setting, which we discuss next.

A. Power Model for Downlink PASS

Using TDMA, the AP transmits K different encoded signals in K time intervals. Let $s_{k,0}$ with power $P_k^{\text{in}} = |s_{k,0}|^2$ denote the signal fed to the waveguide in time interval k at location $x = 0$. The phase-shifted signal that specifies the EM field at location x of the waveguide in this time interval is given by

$$s_k(x) = e^{-j\beta x} s_{k,0}, \quad (1)$$

where $\beta = 2\pi i_{\text{ref}}/\lambda$ with λ being the wavelength.

At pinching element n , the EM wave starts coupling at location $x_{0,n}$ and splits into two components by the end of the complete coupling at x_n : (i) a component that is coupled with the pinching element and radiated in the free space, and (ii) a component that is remained in the waveguide. This power splitting repeats towards the last element on the waveguide and specifies the radiated power on each element [11]. To characterize the power radiation in the PASS, let us start with

the first element. Following the analysis in [11], the signal radiated by the first element is given by

$$s_{k,1} = \sin(\kappa \ell_1) e^{-j\beta x_1} s_{k,0}, \quad (2)$$

for a constant κ that represents the coupling coefficient. The signal-carrying components of the remained wave in the waveguide is further given by

$$s_{k,1}^r = \cos(\kappa \ell_1) e^{-j\beta x_1} s_{k,0}. \quad (3)$$

The signal $s_{k,1}^r$ can be treated as a new input fed at location x_1 , whose splitting at $x_2 - x_1$ specifies the radiation on pinching element 2. By repeating this procedure, we can conclude that the signal radiated by element n in time interval k is [11]

$$s_{k,n} = \sqrt{1 - \delta_n^2} \left(\prod_{i=1}^{n-1} \delta_i \right) e^{-j\beta x_n} s_{k,0}, \quad (4)$$

where $\delta_i = \cos(\kappa \ell_i)$. In the sequel, we refer to δ_i as the *power split coefficient* of element i . For $\boldsymbol{\delta} = [\delta_1, \dots, \delta_N]^T \in [0, 1]^N$, we further define the effective split coefficient n as

$$A_n(\boldsymbol{\delta}) = \sqrt{1 - \delta_n^2} \left(\prod_{i=1}^{n-1} \delta_i \right), \quad (5)$$

and write compactly $s_{k,n} = A_n(\boldsymbol{\delta}) e^{-j\beta x_n} s_{k,0}$, in the sequel.

Considering the EM propagation, the power radiated from the element n in the time interval k is

$$P_{k,n}^{\text{tx}} = A_n^2(\boldsymbol{\delta}) |s_{k,0}|^2 = (1 - \delta_n^2) \left(\prod_{i=1}^{n-1} \delta_i^2 \right) P_k^{\text{in}}. \quad (6)$$

The total transmit power in this interval is thus given by

$$P_k^{\text{tx}} = \sum_{n=1}^N P_{k,n}^{\text{tx}} = P_k^{\text{in}} \sum_{n=1}^N (1 - \delta_n^2) \left(\prod_{i=1}^{n-1} \delta_i^2 \right). \quad (7)$$

Assuming same time duration for all TDMA intervals, the average transmitted power in downlink is given by

$$\bar{P}^{\text{tx}} = \frac{1}{K} \sum_{k=1}^K P_k^{\text{tx}} = \bar{P}^{\text{in}} \sum_{n=1}^N A_n^2(\boldsymbol{\delta}), \quad (8)$$

where $\bar{P}^{\text{in}} = \sum_k P_k^{\text{in}}/K$ is the average input power.

Remark 1: As mentioned, we assume that the remaining power in the waveguide is negligible. In asymmetric architectures, one can set this power to zero by matching the last pinching element, i.e., by setting $\delta_N = \cos(\kappa \ell_N) = 0$. In a symmetric architecture, i.e., $\delta_n = \delta$ for all $n \in [N]$, this is not feasible. However, the remaining power in this case is $\delta^{2N} \bar{P}^{\text{in}}$ which can always set arbitrarily close to zero if the length of the elements (specifying δ) is tuned properly.

In addition to the input power, there is a circuit power consumed by the radio frequency chain deployed to radiate the modulated signal in the waveguide. This is modeled as a single term P^{cir} , as there is a single chain connected to the waveguide. Assuming this term to be fixed, we can model the total power consumed by this PASS as

$$P^{\text{total}} = \bar{P}^{\text{in}} + P^{\text{cir}} = \frac{1}{K} \sum_{k=1}^K P_k^{\text{in}} + P^{\text{cir}}. \quad (9)$$

Note that the consumed power in this case does not scale with the PASS size N . This is indeed intuitive: regardless of N ,

the power consumed by the PASS is specified by the power fed to the waveguide and what is burned in the circuitry.

B. Characterizing Energy Efficiency

Considering EM wave propagation, the signal received by user k at point $\mathbf{u}_k = [x_k^u, y_k^u, z_k^u]$ is given by

$$y_k = \xi_k \sum_{n=1}^N \frac{e^{-j\alpha \mathcal{D}_k(x_n)}}{\mathcal{D}_k(x_n)} s_{k,n} + \varepsilon_k \quad (10)$$

where ε_k is additive Gaussian noise with mean zero and variance σ_k^2 , ξ_k is an attenuation coefficient capturing shadowing, scalar $\alpha = 2\pi/\lambda$ is the wave-number, and $\mathcal{D}_k(x_n)$ denotes the distance between the user and pinching element n , i.e.,

$$\mathcal{D}_k(x_n) = \sqrt{(x_k^u - x_n)^2 + y_k^{u2} + (z_k^u - a)^2}. \quad (11)$$

Let us define $\mathbf{x} = [x_1, \dots, x_N] \in [0, L]^N$. Considering (4), we can write compactly $y_k = h_k(\mathbf{x}, \boldsymbol{\delta}) s_{k,0} + \varepsilon_k$ with

$$h_k(\mathbf{x}, \boldsymbol{\delta}) = \xi_k \sum_{n=1}^N \frac{A_n(\boldsymbol{\delta})}{\mathcal{D}_k(x_n)} e^{-j(\alpha \mathcal{D}_k(x_n) + \beta x_n)}, \quad (12)$$

which describes an effective Gaussian channel from the AP to user k . We can hence write the downlink transmission rate to user k as

$$\mathcal{R}_k(P_k^{\text{in}}, \mathbf{x}, \boldsymbol{\delta}) = \log(1 + \Gamma_k P_k^{\text{in}} G_k(\mathbf{x}, \boldsymbol{\delta})), \quad (13)$$

where $\Gamma_k = \xi_k^2/\sigma_k^2$, and $G_k(\mathbf{x}, \boldsymbol{\delta}) = |h_k(\mathbf{x}, \boldsymbol{\delta})|^2/\xi_k^2$ denotes the *effective channel gain* to user k . Noting that the system operates in TDMA, the spectral efficiency is given by

$$\text{SE}(\mathbf{P}^{\text{in}}, \mathbf{x}, \boldsymbol{\delta}) = \frac{1}{K} \sum_{k=1}^K \mathcal{R}_k(P_k^{\text{in}}, \mathbf{x}, \boldsymbol{\delta}). \quad (14)$$

where $\mathbf{P}^{\text{in}} = [P_1^{\text{in}}, \dots, P_K^{\text{in}}]^T$ is the *user power allocation*.

Considering the power model and spectral efficiency, the EE of the PASS is given by

$$\mathcal{E}(\mathbf{P}^{\text{in}}, \mathbf{x}, \boldsymbol{\delta}) = \frac{\text{SE}(\mathbf{P}^{\text{in}}, \mathbf{x}, \boldsymbol{\delta})}{P_{\text{total}}} \quad (15a)$$

$$= \left(\sum_{k=1}^K \mathcal{R}_k(P_k^{\text{in}}, \mathbf{x}, \boldsymbol{\delta}) \right) \left(\sum_{k=1}^K P_k^{\text{in}} + KP^{\text{cir}} \right)^{-1}. \quad (15b)$$

The expression in (15b) demonstrates two intuitive facts: (i) for a fixed power allocation policy among users, optimizing the EE is equivalent to optimization of the spectral efficiency. This is intuitive, as the radiated power in the PASS is controlled by the position and coupling length of the pinching elements which impact the EE only through spectral efficiency. (ii) For a fixed PASS configuration, i.e., fixed \mathbf{x} and $\boldsymbol{\delta}$, the EE optimization is equivalent to that of conventional TDMA systems. This follows the fact that PASS only provides extra degrees of freedom to modify the communication channel, and does not impact the nature of wave propagation.

III. STATIC AND DYNAMIC DESIGN FOR PASS

The ultimate goal of this work is to develop an algorithmic approach to optimize the EE of this system. This is a *hybrid* design problem in which the signal-level parameters, i.e., user power allocation, and system-level parameters, i.e., location

and coupling length of pinching elements, are designed jointly for optimal EE. One can readily see that the optimal design depends on the system setting, e.g., users' location. Therefore, any algorithmic approach should update the design parameters at a certain rate. While signal-level parameters can be updated at high rate, the update rate of system-level parameters can be limited due to physical restriction.

In this section, we consider two cases; namely, the *dynamic* and *static* designs. The former refers to the case, where PASS physical degrees of freedom can be updated at a high rate, while the latter considers the scenarios, in which the system parameters are updated at significantly lower rate.

A. Dynamic Design of PASS

In dynamic design, we assume that the pinching locations are dynamically tuned at a rate comparable to channel coherence. In other words, the PASS is able to tune the location of its elements, as the users change their locations. Such design can be realized by implementing each element via multiple mechanically shifting coupling units on the waveguide, each covering one part of the waveguide [2], [3].

Although a dynamic change of pinching locations is realistic in slow changing settings, a dynamic tuning of split coefficients δ_n is not feasible in practice, as they are controlled by the coupling length of the elements. We thus formulate the energy-efficient design in a dynamic setting as follows.

Definition 1 (Dynamic EE Design): The dynamic energy-efficient design of PASS solves the following problem

$$\max_{\boldsymbol{\delta}} \mathbb{E}_{\mathbf{u}_1, \dots, \mathbf{u}_K} \left\{ \max_{\mathbf{x}, \mathbf{P}^{\text{in}}} \mathcal{E}(\mathbf{P}^{\text{in}}, \mathbf{x}, \boldsymbol{\delta}) \right\} \quad (D)$$

$$\text{s.t. } \boldsymbol{\delta} \in [0, 1]^N, \mathbf{x} \in \mathbb{L}, \text{ and } \sum_{k=1}^K P_k^{\text{in}} \leq KP_0, \quad (C)$$

for some given P_0 that specifies the limit on the average power radiated by the AP to the waveguide, and \mathbb{L} that is defined as

$$\mathbb{L} = \{ \mathbf{x} \in \mathbb{R}^N : 0 \leq x_n \leq L \text{ and } |x_n - x_{n-1}| \geq \Delta \}, \quad (16)$$

specifying the set of feasible locations on the waveguide.

In the dynamic formulation, the user power allocation and pinching locations are optimized for given user locations, while the split coefficients are designed to maximize the *ergodic* EE, averaged over user locations.

B. Static Design of PASS

In static settings, the update rate of the antenna locations is not in the order of the network coherence. This means that the antenna locations are updated at significantly lower rate as compared to the environmental parameters, e.g. user locations. In this case, the efficient design considers *ergodic* efficiency of the system. An energy-efficient static design for PASS is hence formulated as follows.

Definition 2 (Static EE Design): The static energy-efficient design of PASS solves the following problem

$$\max_{\boldsymbol{\delta}, \mathbf{x}} \mathbb{E}_{\mathbf{u}_1, \dots, \mathbf{u}_K} \left\{ \max_{\mathbf{P}} \mathcal{E}(\mathbf{P}^{\text{in}}, \mathbf{x}, \boldsymbol{\delta}) \right\} \text{ s.t. } (C), \quad (S)$$

for some average power P_0 , and \mathbb{L} given in (16).

Algorithm 1 User Power Allocation

```
1: Initialize  $\lambda \leftarrow 0$ 
2: repeat
  #apply water-filling
3:   Find  $\ell \geq \lambda$  by checking the slackness
4:   Update  $P_k^{\text{in}} \leftarrow \max\{0, 1/\ell - 1/a_k\}$ 
5:   Update  $\mathcal{R} \leftarrow \sum_k \log(1 + a_k P_k^{\text{in}})$  and  $\mathcal{P} \leftarrow \sum_k P_k^{\text{in}}$ 
  #update  $\lambda$ 
6:    $\phi \leftarrow \mathcal{R} - \lambda (K P^{\text{cir}} + \mathcal{P})$ 
7:    $\lambda \leftarrow \mathcal{R} / (K P^{\text{cir}} + \mathcal{P})$ 
8: until  $|\phi| \leq \varepsilon$ 
```

It is worth noting that the key difference between the two designs is the objective with respect to the pinching locations: while a dynamic PASS updates the locations frequently to optimize the *instantaneous* EE, the static PASS tunes its locations to optimize its *ergodic* throughput.

IV. ALGORITHMS FOR DYNAMIC AND STATIC DESIGN

We develop a hybrid algorithmic scheme based on block coordinate descent, which approximates the solution by alternating between marginal problems in δ , \mathbf{P}^{in} and \mathbf{x} . Note that in both designs, we have both dynamic and static variables: δ and \mathbf{P}^{in} are static and dynamic, respectively, while \mathbf{x} changes from dynamic in (\mathcal{D}) to static in (\mathcal{S}). As a result, our scheme is two-tier: the inner-loop updates the dynamic variables, while static variables are updated in an outer loop that is run at the end of a time window including multiple coherence frames.

A. Power Allocation

The user power allocation, i.e. optimization in \mathbf{P}^{in} , is a dynamic program. The marginal problem in this case is specified by treating the other variables as fixed: let $a_k = \Gamma_k G_k(\mathbf{x}, \delta)$. Then, the power allocation task reduces to

$$\max_{\mathbf{P}^{\text{in}}} \frac{\sum_k \log(1 + a_k P_k^{\text{in}})}{K P^{\text{cir}} + \sum_k P_k^{\text{in}}} \text{ s.t. } \sum_k P_k^{\text{in}} \leq P_0. \quad (\mathcal{M}_1)$$

The marginal problem in (\mathcal{M}_1) describes a standard EE maximization, whose solution is given by Dinkelbach method [13]. Starting from an initial $\lambda \in \mathbb{R}$, we iterate as follows:

1) For a fixed λ , solve

$$\max_{\mathbf{P}^{\text{in}}} \left[\sum_k \log(1 + a_k P_k^{\text{in}}) - \lambda P_k^{\text{in}} \right] \text{ s.t. } \sum_k P_k^{\text{in}} \leq P_0.$$

2) Use the solution of Step 1 to update λ as

$$\lambda \leftarrow \frac{\sum_k \log(1 + a_k P_k^{\text{in}})}{K P^{\text{cir}} + \sum_k P_k^{\text{in}}}.$$

The solution to the optimization in Step 1 is given by water-filling. The power allocation algorithm describes an iterative water-filling, as summarized in Algorithm 1.

B. PASS Tuning

The PASS tuning problem, i.e. optimization in \mathbf{x} , changes from dynamic in (\mathcal{D}) to static in (\mathcal{S}). We hence discuss the marginal problem of each design separately in the sequel.

Algorithm 2 Pinching Location Tuning

```
1: Initialize  $\mathbf{x} \in \mathbb{L}$  and a grid set  $\mathbb{G}$  on  $[0, L]$ 
2: for  $r = 1 : N$  do
3:   Find  $f_{k,r}(x)$  and compute  $\mathbb{F} = \{F_r(x) : x \in \mathbb{G}\}$ 
4:   Update  $x_r \leftarrow \operatorname{argmax} \mathbb{F}$ 
5:   while there is  $n < r$  such that  $|x_r - x_n| < \Delta$  do
6:     Update  $\mathbb{F} = \mathbb{F} - \{F_r(x_r)\}$  and  $x_r \leftarrow \operatorname{argmax} \mathbb{F}$ 
7:   end while
8: end for
9:  $\mathbf{x} \leftarrow \operatorname{sort} [x_1, \dots, x_N]$ 
```

Dynamic Case: In dynamic design, for fixed \mathbf{P}^{in} and δ , we marginally solve

$$\max_{\mathbf{x} \in \mathbb{L}} \sum_k \log(1 + \Gamma_k P_k^{\text{in}} G_k(\mathbf{x}, \delta)). \quad (\mathcal{M}_2^{\mathcal{D}})$$

Due to the extreme fluctuation on the objective surface, the classical gradient decent leads to an unreliable solution to ($\mathcal{M}_2^{\mathcal{D}}$). We therefore solve this problem via Gauss-Seidel approach: let $x_r = x$ denote the location of element r . Starting with $r = 1$, we update x_r , while treating the other elements as fixed. In this case, $G_k(\mathbf{x}, \delta)$ is given in terms of x_r as

$$G_k(\mathbf{x}, \delta) = f_{k,r}(x) = \left| \tau_{k,r} + \frac{A_r(\delta)}{\mathcal{D}_k(x)} e^{-j(\alpha \mathcal{D}_k(x) + \beta x)} \right|^2, \quad (17)$$

where $\tau_{k,r}$ is given by

$$\tau_{k,r} = \sum_{n \neq r} \frac{A_n(\delta)}{\mathcal{D}_k(x_n)} e^{-j(\alpha \mathcal{D}_k(x_n) + \beta x_n)}. \quad (18)$$

Replacing in ($\mathcal{M}_2^{\mathcal{D}}$), the tuning of element r reduces to optimizing the scalar objective

$$F_r(x) = \sum_k \log(1 + \Gamma_k P_k^{\text{in}} f_{k,r}(x)), \quad (19)$$

which can be addressed by search on a fine grid. The final algorithm is summarized in Algorithm 2.

Static Case: The PASS tuning in the static design reduces to the following marginal optimization

$$\max_{\mathbf{x} \in \mathbb{L}} \mathbb{E}_{\mathbf{u}_1, \dots, \mathbf{u}_K} \left\{ \frac{\sum_k \log(1 + \Gamma_k P_k^{\text{in}} G_k(\mathbf{x}, \delta))}{K P^{\text{cir}} + \sum_k P_k^{\text{in}}} \right\}. \quad (\mathcal{M}_2^{\mathcal{S}})$$

It is worth noting that unlike the dynamic case, this optimization is not generally equivalent to SE maximization, since the power allocation is dynamically changing.

Assuming that the coherence interval of the system, i.e. number of transmission frames, per which the location of the elements is optimized once, contains m samples of locations $\mathbf{u}_{k,1}, \dots, \mathbf{u}_{k,m}$ for user k , we can estimate the ergodic EE as

$$\hat{\mathcal{E}}(\mathbf{x}) = \frac{1}{m} \sum_{i=1}^m \frac{\sum_k \log(1 + \Gamma_k P_{k,i}^{\text{in}} G_{k,i}(\mathbf{x}, \delta))}{K P^{\text{cir}} + \sum_k P_{k,i}^{\text{in}}}, \quad (20)$$

where $G_{k,i}(\mathbf{x}, \delta)$ and $P_{k,i}^{\text{in}}$ denote the channel gain in sample location $\mathbf{u}_{k,i}$ and its corresponding dynamic power allocation.

Using the estimate $\hat{\mathcal{E}}(\mathbf{x})$, ($\mathcal{M}_2^{\mathcal{S}}$) is approximately solved by

$$\max_{\mathbf{x} \in \mathbb{L}} \hat{\mathcal{E}}(\mathbf{x}), \quad (\hat{\mathcal{M}}_2^{\mathcal{S}})$$

which is solved via the Gauss-Seidel approach: defining

$$f_{k,r,i}(x) = \left| \tau_{k,r,i} + \frac{A_r(\boldsymbol{\delta})}{\mathcal{D}_{k,i}(x)} e^{-j(\alpha \mathcal{D}_{k,i}(x) + \beta x)} \right|^2, \quad (21)$$

with $\tau_{k,r,i}$ being

$$\tau_{k,r,i} = \sum_{n \neq r} \frac{A_n(\boldsymbol{\delta})}{\mathcal{D}_{k,i}(x_n)} e^{-j(\alpha \mathcal{D}_{k,i}(x_n) + \beta x_n)}, \quad (22)$$

we compute the scalar objective for element r as

$$F_r(x) = \frac{1}{m} \sum_{i=1}^m \frac{1}{P_i^{\text{sum}}} \sum_k \log(1 + \Gamma_k P_{k,i}^{\text{in}} f_{k,r,i}(x)), \quad (23)$$

where P_i^{sum} is defined as

$$P_i^{\text{sum}} = K P^{\text{cir}} + \sum_k P_{k,i}^{\text{in}}. \quad (24)$$

We solve each scalar problem by a linear search on a fine grid.

C. Tuning Coupling Length

The coupling tuning is performed statically by solving

$$\max_{\boldsymbol{\delta}} \mathbb{E}_{\mathbf{u}_1, \dots, \mathbf{u}_K} \left\{ \frac{\sum_k \log(1 + \Gamma_k P_{k,i}^{\text{in}} G_k(\mathbf{x}, \boldsymbol{\delta}))}{K P^{\text{cir}} + \sum_k P_k^{\text{in}}} \right\}. \quad (\mathcal{M}_3)$$

The objective in this case is a well-defined function in $\boldsymbol{\delta}$, and hence we can address this task by gradient ascent.

Similar to the static design of PASS, we assume that we have m samples of user locations in a coherence interval. Let the user allocation vector and antenna locations at sample i be \mathbf{P}_i^{in} and \mathbf{x}_i , respectively. Note that in the dynamic location tuning $\mathbf{x}_i \neq \mathbf{x}_j$ in general for two samples $i \neq j$, while in the static case, $\mathbf{x}_1 = \dots = \mathbf{x}_m$. The objective is then estimated as

$$\hat{\mathcal{E}}(\boldsymbol{\delta}) = \frac{1}{m} \sum_{i=1}^m \frac{1}{P_i^{\text{sum}}} \sum_k \log(1 + \Gamma_k P_{k,i}^{\text{in}} G_{k,i}(\mathbf{x}_i, \boldsymbol{\delta})). \quad (25)$$

This defines a smooth function in $\boldsymbol{\delta}$, whose maximum is tracked via gradient ascent. To this end, we write

$$\nabla \hat{\mathcal{E}} = \frac{1}{m} \sum_{i=1}^m \frac{1}{P_i^{\text{sum}}} \sum_k \frac{\Gamma_k P_{k,i}^{\text{in}} \nabla G_{k,i}(\mathbf{x}_i, \boldsymbol{\delta})}{1 + \Gamma_k P_{k,i}^{\text{in}} G_{k,i}(\mathbf{x}_i, \boldsymbol{\delta})}. \quad (26)$$

Using chain rule, $\nabla G_{k,i}(\mathbf{x}_i, \boldsymbol{\delta}) = 2\Re \left\{ \Xi_{k,i}^*(\boldsymbol{\delta}) \nabla \Xi_{k,i}(\boldsymbol{\delta}) \right\}$, where we define

$$\Xi_{k,i}(\boldsymbol{\delta}) = \sum_r \eta_{k,r,i} A_r(\boldsymbol{\delta}) \quad (27)$$

with $\eta_{k,n,i}$ being

$$\eta_{k,n,i} = \frac{e^{-j(\alpha \mathcal{D}_{k,i}(x_{i,n}) + \beta x_{i,n})}}{\mathcal{D}_{k,i}(x_{i,n})}. \quad (28)$$

The gradient of $\Xi_{k,i}(\boldsymbol{\delta})$ is further computed in terms of the gradient of $A_n(\boldsymbol{\delta})$ using the identity

$$\frac{\nabla A_n(\boldsymbol{\delta})}{A_n(\boldsymbol{\delta})} = \left[\frac{1}{\delta_1}, \dots, \frac{1}{\delta_{n-1}}, -\frac{\delta_n}{1 - \delta_n^2}, 0, \dots, 0 \right]^\top. \quad (29)$$

Using the above derivation, the local maximizer is determined by tracking the gradient. Nevertheless, using the vanilla gradient ascent, the coupling coefficients can be update to invalid values, i.e., $\delta_n \notin [0, 1]$. To this end, we further project the update $\boldsymbol{\delta}$ to the feasible region after each update. This concludes the iterative algorithm in Algorithm 3.

Algorithm 3 Coupling Tuning

- 1: Initialize $\boldsymbol{\delta} \in [0, 1]^N$ and choose a small step size μ
- 2: **repeat**
- 3: Compute $G_{k,i}(\mathbf{x}_i, \boldsymbol{\delta})$ and $\nabla G_{k,i}(\mathbf{x}_i, \boldsymbol{\delta})$ at $\boldsymbol{\delta}$
- 4: Update $\boldsymbol{\delta} \leftarrow \boldsymbol{\delta} + \mu \nabla \hat{\mathcal{E}}$
- 5: **for** $n = 1 : N$ **do**
- 6: **if** $\delta_n > 1$ **then** Set $\delta_n = 1$
- 7: **else if** $\delta_n < 0$ **then** Set $\delta_n = 0$
- 8: **end if**
- 9: **end for**
- 10: **until** it converges

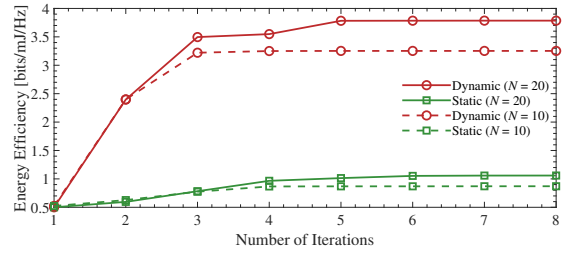


Fig. 1: Convergence of the proposed algorithms.

V. NUMERICAL EXPERIMENT

We next validate the proposed designs through numerical experiments and compare it against the baseline. Unless stated otherwise, $K = 6$ users are randomly and uniformly distributed within a rectangular service region of size $D_x = 50$ m and $D_y = 20$ m, centered at $[D_x/2, 0, 0]$. The waveguide is aligned along the x -axis, deployed at a height of $a = 3$ m, and covers the entire service area. The parameters of the simulation setup are summarized as follows: carrier frequency is $f_c = 28$ GHz, effective refractive index is $i_{\text{ref}} = 1.4$, circuit power is set to $P^{\text{cir}} = 0$ dBm, grid search resolution is $Q = 10^4$, minimum inter-antenna distance is set to $\Delta = \lambda/2$, and noise variance is $\sigma_k^2 = -90$ dBm. In iterative algorithms, user powers are initialized as $P_k^{\text{in}} = P/K$ for a total power P , the splitting coefficients are set to $\delta_n = 0.5$ for $n \in [N]$, and the initial pinching locations are uniformly distributed, i.e. $x_n = (n-1)D_x/N - 1$. For comparison, we evaluate the proposed coupling-length-tunable PASS against a baseline configuration where all antennas employ a fixed power-splitting coefficient of $\delta_n = 0.5$ for $n \in [N]$.

Fig. 1 illustrates the convergence behavior of the proposed algorithmic scheme for both dynamic and static designs under different numbers of antenna elements N . As observed, the EE increases with the number of iterations and converges to a stable value, confirming the convergence and effectiveness of the proposed methods. Moreover, the dynamic design achieves considerably higher EE than the static design. This observation is intuitive, as the dynamic approach adaptively optimizes the antenna placement within each coherence interval.

Fig. 2 shows the EE against the maximum transmit power P . For completeness, both EE-oriented and SE-oriented designs are evaluated, where the latter uses the proposed frame-

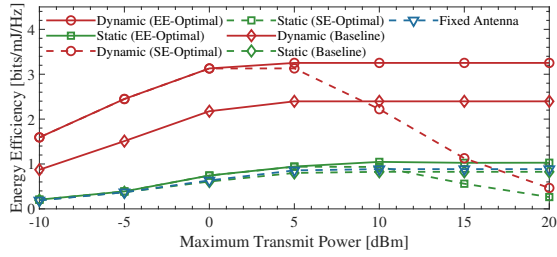


Fig. 2: EE vs the transmit power at $N = 10$.

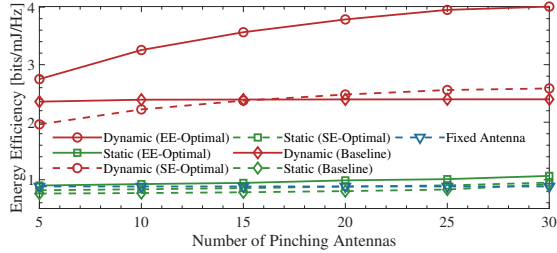


Fig. 3: EE vs the number of elements at $P_0 = 10$ dBm.

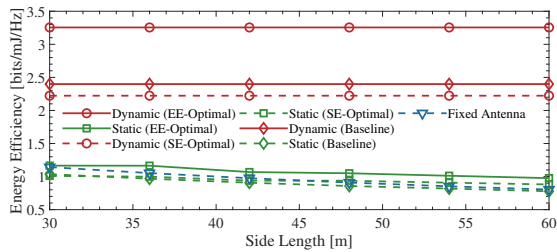


Fig. 4: EE vs the side length D_x at $P_0 = 10$ dBm and $N = 10$.

work to directly maximize the SE. As shown, for both dynamic and static configurations, the EE-oriented design achieves higher EE than the SE-oriented counterpart, particularly in the high-SNR regime. Furthermore, the dynamic design outperforms the static one due to its ability to adaptively optimize the pinching-antenna placement for each user location. This highlights the critical role of antenna placement in enhancing system efficiency. In addition, when compared with the baseline scheme employing a fixed coupling length, the proposed PASS design with tunable coupling length significantly improves the EE especially under dynamic design, which validates the effectiveness of adaptive coupling-length control in improving system performance. For reference, the results for a conventional fixed-position antenna located at the center of the service region are also included. Although the static design avoids frequent updates of antenna positions, its performance gain over traditional fixed-antenna systems remains limited, underscoring the importance of spatial adaptability in PASS.

Fig. 3 plots the EE as a function of the number of antennas. The figure shows that for the proposed designs, the achievable EE increases steadily with the antenna number. In contrast, for the PASS design with tunable coupling length, the EE exhibits only marginal improvement as the number of antennas grows. This occurs because, under fixed coupling length, most of the radiated energy is emitted by the first few antennas, and thus adding more antennas contributes little to overall

system efficiency. Finally, in Fig. 4, we plot the EE against the side length D_x . For the dynamic design, the antenna placement is optimized individually for each user within its allocated time slot. This allows the system to maintain nearly constant EE even when users are distributed over a wider area. In contrast, the static design optimizes antenna placement based on the overall user distribution, and its achievable EE decreases as D_x increases. This degradation arises, since the average user-to-antenna distance becomes larger with a wider service region, which leads to higher path loss.

VI. CONCLUSIONS

This work formulated the EE of PASSs considering their EM characteristics. Unlike conventional movable-antenna technologies, the per-element power distribution in PASSs is not controlled explicitly through an allocation policy, but only implicitly through the pinching locations and couplings. We developed static and dynamic algorithms for EE maximization in PASSs. While the proposed designs outperform the baseline in both cases, dynamic tuning of pinching elements enables the PASS to significantly boost the throughput, as compared with the baseline. This suggests that PASSs can operate significantly energy-efficient in scenarios with slow fluctuations in the network, e.g. indoor environments with low user mobility. Extending the proposed EE formulation to MIMO settings is a natural direction for future work, which is currently ongoing.

REFERENCES

- [1] A. Fukuda, H. Yamamoto, H. Okazaki, Y. Suzuki, and K. Kawai, "Pinching antenna: Using a dielectric waveguide as an antenna," *NTT DOCOMO Technical J.*, vol. 23, no. 3, pp. 5–12, 2022.
- [2] Z. Ding, R. Schober, and H. Vincent Poor, "Flexible-antenna systems: A pinching-antenna perspective," *IEEE Trans. Commun.*, pp. 1–1, 2025.
- [3] Y. Liu, Z. Wang, X. Mu, C. Ouyang, X. Xu, and Z. Ding, "Pinching-antenna systems: Architecture designs, opportunities, and outlook," *IEEE Communications Magazine*, pp. 1–7, 2025.
- [4] C. Ouyang, Z. Wang, Y. Liu, and Z. Ding, "Array gain for pinching-antenna systems (PASS)," 2025, arXiv preprint arXiv:2501.05657.
- [5] A. Beryhi, C. Ouyang, S. Asaad, Z. Ding, and H. V. Poor, "Downlink beamforming with pinching-antenna assisted MIMO systems," in *Proc. IEEE Int. Conf. Commun. Workshop (ICC Workshop)*, 2025, pp. 1–7.
- [6] —, "MIMO-PASS: Uplink and downlink transmission via MIMO pinching-antenna systems," 2025, arXiv preprint arXiv:2503.03117.
- [7] D. Tyrovolas, S. A. Tegos, P. D. Diamantoulakis, S. Ioannidis, C. K. Liaskos, and G. K. Karagiannidis, "Performance analysis of pinching-antenna systems," *IEEE Trans. Cogn. Commun. Net.*, pp. 1–1, 2025.
- [8] S. Shan, C. Ouyang, Y. Li, and Y. Liu, "Secure multicast communications with pinching-antenna systems (PASS)," 2025, arXiv preprint arXiv:2509.16045.
- [9] X. Xie, Y. Lu, and Z. Ding, "Graph neural network enabled pinching antennas," *IEEE Wireless Commun. Lett.*, vol. 14, no. 9, pp. 2982–2986, 2025.
- [10] M. Zeng, J. Wang, G. Zhou, F. Fang, and X. Wang, "Energy-efficient design for downlink pinching-antenna systems with QoS guarantee," 2025, arXiv preprint arXiv:2505.14904.
- [11] Z. Wang, C. Ouyang, X. Mu, Y. Liu, and Z. Ding, "Modeling and beamforming optimization for pinching-antenna systems," 2025, arXiv preprint arXiv:2502.05917.
- [12] W. Mei, X. Wei, B. Ning, Z. Chen, and R. Zhang, "Movable-antenna position optimization: A graph-based approach," *IEEE Wireless Commun. Lett.*, vol. 13, no. 7, pp. 1853–1857, Jul. 2024.
- [13] R. S. Prabhu and B. Daneshrad, "An energy-efficient water-filling algorithm for OFDM systems," in *Proc. IEEE Int. Conf. Commun. (ICC)*, 2010, pp. 1–5.